DDR

DRUG DEVELOPMENT RESEARCH 71 : 240–248 (2010)

Research Article

Econazole-Induced Ca^{2+} Fluxes and Apoptosis in Human Oral Cancer Cells

Daih-Huang Kuo,[1]* Li-Min Liu,[1] Hsin-Wei Chen,[1] Fu-An Chen,[1] and Chung-Ren Jan[2]

[1]*Graduate Institute of Pharmaceutical Science and Department of Pharmacy, Tajen University, Pingtung, Taiwan*

[2]*Department of Medical Education and Research, Kaohsiung Veterans General Hospital, Kaohsiung, Taiwan*

Strategy, Management and Health Policy				
Enabling Technology, Genomics, Proteomics	Preclinical Research	Preclinical Development Toxicology, Formulation Drug Delivery, Pharmacokinetics	Clinical Development Phases I-III Regulatory, Quality, Manufacturing	Postmarketing Phase IV

ABSTRACT The effect of econazole on cytosolic free Ca^{2+} concentrations ($[Ca^{2+}]_i$) and viability was explored in human oral cancer cells (OC2), using the fluorescent dyes fura-2 and WST-1, respectively. Econazole at concentrations of >1 μM increased $[Ca^{2+}]_i$ in a concentration-dependent manner. The Ca^{2+} signal was reduced partly by removing extracellular Ca^{2+}. The econazole-induced Ca^{2+} influx was sensitive to blockade of aristolochic acid (phospholipase A_2 inhibitor) and GF109203X (PKC inhibitor). In Ca^{2+}-free medium, after treatment with 1 μM thapsigargin (an endoplasmic reticulum Ca^{2+} pump inhibitor), 30 μM econazole failed to induce a $[Ca^{2+}]_i$ rise. Inhibition of phospholipase C with 2 μM U73122 substantially suppressed econazole-induced $[Ca^{2+}]_i$ rise. At concentrations of 5–70 μM econazole killed cells in a concentration-dependent manner. The cytotoxic effect of 50 μM econazole was enhanced by prechelating cytosolic Ca^{2+} with 1,2-bis(2-aminophenoxy)ethane-N,N,N′,N′-tetraacetic acid (BAPTA). The ERK MAPK inhibitor, PD98059 (10 μM), also enhanced 20 μM econazole-induced cell death. Propidium iodide staining data suggest that econazole induced apoptosis between concentrations of 10–70 μM. Collectively, in OC2 cells, econazole induced $[Ca^{2+}]_i$ rises by causing Ca^{2+} release from the endoplasmic reticulum and Ca^{2+} influx from phospholipase A_2/PKC-regulated Ca^{2+} channels. Furthermore, econazole caused cell death appeared to be regulated by ERK MAPK. Drug Dev Res 71:240–248, 2010.

Key words: apoptosis; Ca^{2+}; econazole; OC2 cells; oral cancer

INTRODUCTION

Econazole is a widely used antifungal drug for the treatment of keratitis and athlete's foot [Vanden Bossche et al., 2003; Florcruz and Peczon, 2008]. Econazole is also used as a pharmacological tool to inhibit store-operated Ca^{2+} entry [Mason et al., 1993; Jiang et al., 2006; Davies et al., 2004], a Ca^{2+} influx that is induced by depletion of internal Ca^{2+} [Salido et al., 2009]. Although econazole and other agents were thought to inhibit cytochrome P-450 [McLean et al., 2002], evidence from HL-60 cells showed that cytochrome P-450 was not involved in the effect of econazole on Ca^{2+} influx [Koch et al., 1994]. Paradoxically, some reports performed in different cell lines have shown that econazole could induce a rise in

Grant sponsor: Veterans General Hospital-Kaohsiung; Grant number: VGHKS98–100.

*Correspondence to: Daih-Huang Kuo, Graduate Institute of Pharmaceutical Science and Department of Pharmacy, Tajen University, Pingtung, Taiwan 907. E-mail: kuo0939@gmail.com

Received 25 December 2009; Accepted 23 February 2010

Published online in Wiley InterScience (www.interscience.wiley.com). DOI: 10.1002/ddr.20366

cytosolic Ca^{2+} level ($[Ca^{2+}]_i$) via induction of Ca^{2+} influx and release of store Ca^{2+} [Jan et al., 1999a; Chang et al., 2005]; however, the effects of econazole on the viability of these cells was unknown. In human colon cancer cells, econazole induced G0/G1 cell cycle arrest via caspase 8-independent apoptotic signaling pathways [Ho et al., 2005]. Furthermore, Zisterer et al. [1997] showed that econazole and other imidazole compounds affect steroidogenesis in Y1 cells and also induced apoptosis in mouse lymphoma and human T-cell leukemia cells via regulation by Bcl-2 and Ca^{2+} [Sobecks et al., 1996].

Jacobsen et al. [1999] showed that cyclodextrin inclusion complexes of antimycotics (containing econazole) intended to act in the oral cavity had a potential for toxicity in TR146 oral epithelial cell with an unknown mechanism. In the present study, we examined the effects of econazole on $[Ca^{2+}]_i$ and viability in the human oral cancer cell line, OC2. A rise in $[Ca^{2+}]_i$ is a key signal for many pathophysiological processes in cells, including apoptosis, lipid peroxidation, radical oxygen species (ROS) generation, and mitochondrial integrity [Berridge, 2006]. However, an abnormal $[Ca^{2+}]_i$ rise was cytotoxic, leading to apoptosis, protein dysfunction, interference of ion flux, etc. [Orrenius and Nicotera, 1994]. The OC2 human oral cancer cell line is a useful model for oral cancer research in which $[Ca^{2+}]_i$ can increase in response to the stimulation of tamoxifen [Chu et al., 2007] and sarfole [Huang et al., 2005].

Using fura-2 as a fluorescent Ca^{2+}-sensitive dye, here we demonstrate that econazole induced $[Ca^{2+}]_i$ rises both in the presence and absence of extracellular Ca^{2+} in OC2 cells. These $[Ca^{2+}]_i$ rises were characterized and concentration-response relationships established with the pathways underlying econazole-induced Ca^{2+} influx and Ca^{2+} release being evaluated. The effect of econazole on cell viability, apoptosis, and the relationship to Ca^{2+} was also explored.

MATERIALS AND METHODS

Cell Culture

OC2 cells obtained from the American Type Culture Collection (ATCC) were cultured in Dulbecco's modified Eagle medium (DMEM) supplemented with 10% heat-inactivated fetal bovine serum (FBS), 100 U/ml penicillin, and 100 μg/ml streptomycin.

Chemicals

The reagents for cell culture were from Gibco (Gaithersburg, MD). Fura-2/AM and 1,2-bis(2-aminophenoxy)ethane-N,N,N′,N′-tetraacetic acid (BAPTA) in ester form were from Molecular Probes (Eugene, OR). Econazole, propidium iodide, and other reagents were from Sigma-Aldrich (St. Louis, MO).

Solutions

Econazole was dissolved in DMSO as a 1 M stock solution. The other agents were dissolved in water, ethanol or DMSO. The concentration of organic solvents in the solution used in experiments did not exceed 0.1%, and did not alter basal $[Ca^{2+}]_i$ or viability.

$[Ca^{2+}]_i$ Measurements

Confluent cells grown on 6-cm dishes were trypsinized and made into a suspension in culture medium at a density of 10^6/ml. Cells were subsequently loaded with 2 μM fura-2/AM for 30 min at 25°C in the same medium. After loading, cells were washed with Ca^{2+}-containing medium twice and made into a suspension in Ca^{2+}-containing medium at a density of 10^7/ml. Fura-2 fluorescence measurements were performed in a water-jacketed cuvette (25°C) with continuous stirring; the cuvette contained 1 ml of medium and 0.5 million cells. Fluorescence was monitored with a Shimadzu RF-5301PC spectrofluorophotometer immediately after 0.1 ml cell suspension was added to 0.9 ml Ca^{2+}-containing or Ca^{2+}-free medium, by recording excitation signals at 340 nm and 380 nm and the emission signal at 510 nm at 1-s intervals. During recording, reagents were added to the cuvette by pausing the recording for 2 s to open and close the cuvette-containing chamber. For calibration of $[Ca^{2+}]_i$, after completion of the experiments, the detergent Triton X-100 and 5 mM $CaCl_2$ were added to the cuvette to obtain the maximal fura-2 fluorescence. The Ca^{2+} chelator EGTA (10 mM) was subsequently added to chelate Ca^{2+} in the cuvette to obtain the minimal fura-2 fluorescence. $[Ca^{2+}]_i$ was calculated as described [Grynkiewicz et al., 1985]. Mn^{2+} quench of fura-2 fluorescence was performed in Ca^{2+}-containing medium containing 50 μM $MnCl_2$. $MnCl_2$ was added to cell suspension in the cuvette 1 min before starting the fluorescence recoding. Data were recorded at excitation signal at 360 nm (Ca^{2+}-insensitive) and emission signal at 510 nm at 1-s intervals as described previously [Merritt et al., 1989].

Cell Viability Assays

Measurement of cell viability was based on the ability of cells to cleave tetrazolium salts by dehydrogenase activity. Augmentation in the amount of developed color directly correlated with the number of live cells. Assays were performed according to manufacturer instructions for this assay (Roche Molecular Biochemical, Indianapolis, IN). Cells were seeded in 96-well plates at a density of 10,000 cells/well in culture medium for 24 h in

the presence of 070 μM econazole. The cell viability detecting reagent 4-[3-[4-lodophenyl]-2-4(4-nitrophenyl) -2H-5-tetrazolio-1,3-benzene disulfonate] (WST-1; 10 μl pure solution) was added to samples after econazole treatment, and cells were incubated for 30 min after the addition of WST-1 in a humidified atmosphere. In experiments using BAPTA/AM to chelate cytosolic Ca^{2+}, fura-2-loaded cells were treated with 5 μM BAPTA/AM for 1 h prior to incubation with 50μ M econazole. Cells were washed once with Ca^{2+}-containing medium and incubated with or without 50 μM econazole in culture medium for 24 h. The absorbance of samples (A_{450}) was determined using enzyme-linked immunosorbent assay (ELISA) reader. Excitation wavelength was 450 nm. Reference wavelength was 690 nm. Blanks were always included in the test. Absolute optical density was normalized to the absorbance of unstimulated cells in each plate and expressed as a percentage of the control value. Absolute optical density induced by treatments with different concentrations of econazole was divided by the absorbance of unstimulated cells (control) in each plate and was expressed as a percentage of the control value. Each group contained 6 replicates (well) and the experiments were repeated three times.

Measurements of Subdiploidy Nuclei by Flow Cytometry

This protocol was based on a previous report [Lovborg et al., 2005]. Cells were seeded in 96-well plates at a density of 10,000 cells/well in culture medium. After treatment with 0–70 μM econazole for 24 h, cells were collected from the media, and were washed with ice-cold Ca^{2+}-containing medium twice and resuspended in 3 ml of 70% ethanol at −20°C. The cells were centrifuged for 5 min at 200 *g*. Ethanol was decanted and the cell pellet was washed with ice-cold medium twice, and was suspended in 1 ml propidium iodide solution (1% Triton X-100, 20 μg propidium iodide, 0.1 mg/ml RNase). The cell pellet was incubated in the dark for 30 min at room temperature. Cell fluorescence was measured in the FACScan flow cytometer (Becton Dickinson Immunocytometry Systems, San Jose, CA), and the data were analyzed using the MODFIT software.

Statistics

Data were analyzed by two-way analysis of variance (ANOVA) using the Statistical Analysis System (SAS®, SAS Institute, Cary, NC). Multiple comparisons between group means were performed by post hoc analysis using the Tukey's honestly significant difference (HSD) procedure. A *P*-value of <0.05 was considered significant.

RESULTS

Effect of Econazole on $[Ca^{2}+]_i$Econazole at concentrations of >1 μM increased $[Ca^{2+}]_i$ in a concentration-dependent manner in Ca^{2+}-containing medium. Figure 1A shows the effects of 1, 5, 10, 20, and 30 μM econazole. At a concentration of 0.1 μM, econazole had no effect on $[Ca^{2+}]_i$. The $[Ca^{2+}]_i$ rise induced by 30 μM econazole was 182 ± 2 nM ($n = 3$; baseline subtracted) at the 74-s time point followed by a sustained phase. At a concentration of 50 μM, econazole induced a similar response to that of 30 μM (not shown). Figure 1C (filled circles) shows the concentration-response curve of the econazole response. The estimated EC_{50} value was ~13 μM.

Further experiments were performed to determine the relative contribution of extracellular Ca^{2+} influx and intracellular Ca^{2+} release in the econazole-induced $[Ca^{2+}]_i$ rises. The $[Ca^{2+}]_i$ rise induced by 30 μM econazole in Ca^{2+}-free medium is shown in Figure 1B (time points of 30–250 s). Removal of extracellular Ca^{2+} did not alter the baseline, suggesting that the amount of leaked fura-2 from the cells was insignificant. Econazole increased $[Ca^{2+}]_i$ by 95 ± 1 nM ($n = 3$) above baseline followed by a slow decay. At 30 μM, econazole-induced $[Ca^{2+}]_i$ rise was reduced by 30% ($P < 0.05$) in the maximum value by removal of extracellular Ca^{2+}.

Effect of Econazole on $Mn^{2}+$ Influx

Experiments were performed to exclude the possibility that the smaller econazole-induced response in Ca^{2+}-free medium was caused by 0.3 mM EGTA-induced acute depletion of intracellular Ca^{2+}. Mn^{2+} enters cells through similar pathways as Ca^{2+} but quenches fura-2 fluorescence at all excitation wavelengths [Merritt et al., 1989]. Thus, quench of fura-2 fluorescence excited at the Ca^{2+}-insensitive excitation wavelength of 360 nm by Mn^{2+} indicates Ca^{2+} influx. Figure 2 shows that in Ca^{2+}-containing medium, 30 μM econazole induced an immediate decrease in the 360-nm excitation signal (compared with control). This suggests that the econazole-induced $[Ca^{2+}]_i$ rise involved Ca^{2+} influx from extracellular space. The decrease attained to a maximum of 71 ± 2 ($n = 3$) arbitrary units at 230 s.

Effect of Aristolochic Acid and GF 109203X on Econazole-Induced $[Ca^{2+}]_i$ Rise

Experiments were performed to explore the regulation of econazole-induced Ca^{2+} signal. La^{3+} (50 μM), Ni^{2+} (10 μM), nifedipine (1 μM), verapamil (1 μM), SK&F96365 (2 μM; store-operated Ca^{2+} entry inhibitor), H-89 (10 μM; PKA [PKA] inhibitor), propranolol (100 μM; phospholipase D inhibitor), and phorbol 12-myristate 13-acetate (PMA; 10 nM, PKC

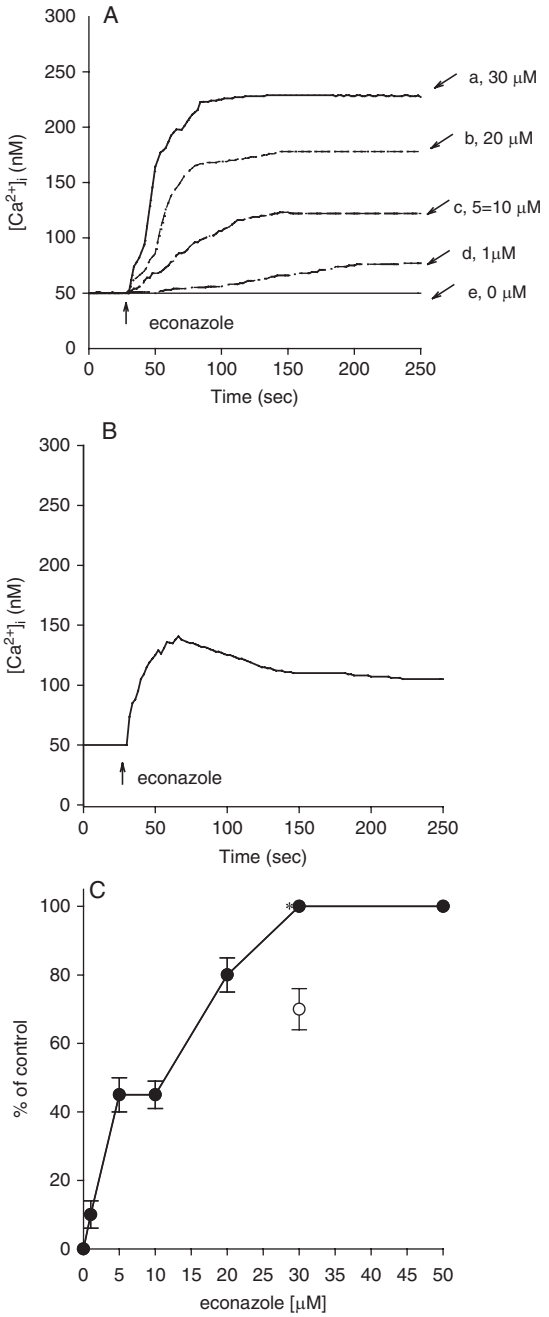

Fig. 1. **A:** Effect of econazole on $[Ca^{2+}]_i$ in fura-2-loaded OC2 cells. Econazole was added at 25 s. The concentration of econazole is indicated. The experiments were performed in Ca^{2+}-containing medium. **B:** Effect of removal of Ca^{2+} on 30 μM econazole-induced $[Ca^{2+}]_i$ rise. Experiments were performed in Ca^{2+}-free medium (Ca^{2+} was replaced with 0.3 mM EGTA). **C:** Concentration-response plot of econazole-induced $[Ca^{2+}]_i$ rise in the presence (filled circles) of extracellular Ca^{2+}. Y axis is the percentage of control, which is the net (baseline subtracted) area under the curve (25–250 s) of the $[Ca^{2+}]_i$ rise induced by 30 μM econazole. The effect of 30 μM econazole in Ca^{2+}-free medium is also shown (open circle). Data are typical of three experiments. $^*P<0.05$ compared with the filled circle (30 μM).

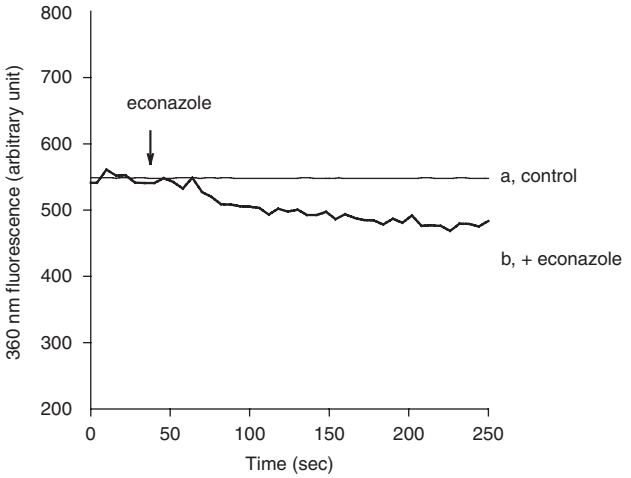

Fig. 2. Effect of econazole on Ca^{2+} influx by measuring Mn^{2+} quench of fura-2 fluorescence. Experiments were performed in Ca^{2+}-containing medium. $MnCl_2$ (50 μM) was added to cells 1 min before fluorescence measurements. The *y* axis is fluorescence intensity (in arbitrary units) measured at the Ca^{2+}-insensitive excitation wavelength of 360 nm and the emission wavelength of 510 nm. Upper trace (a): control; no econazole was present. Lower trace (b): 30 μM econazole was added as indicated. Data are typical of three experiments.

[PKC] activator) failed to alter 30 μM econazole-induced Ca^{2+} signal in the presence of extracellular Ca^{2+}. Conversely, the phospholipase A_2 inhibitor aristolochic acid (20 μM) and the PKC inhibitor GF 109203X (2 μM) inhibited 30 μM econazole-induced $[Ca^{2+}]_i$ rise (Fig. 3).

Internal Ca^{2+} Stores for Econazole-Induced $[Ca^{2+}]_i$ Rises

Previous reports show that the endoplasmic reticulum is a major Ca^{2+} store in most cells [Heath-Engel et al., 2008; Rizzuto et al., 2009]. Figure 4 shows that after treatment with 1 μM thapsigargin, an inhibitor of the endoplasmic reticulum Ca^{2+} pump [Thastrup et al., 1990], for 380 s, the addition of 30 μM econazole failed to induce a $[Ca^{2+}]_i$ rise, compared with the control econazole response shown in Figure 1B.

Involvement of Phospholipase C in Econazole-Induced $[Ca^{2+}]_i$ Rise

As econazole was able to release Ca^{2+} from the endoplasmic reticulum, the role of phospholipase C in this release was examined. U73122, a phospholipase C inhibitor [Thompson et al., 1991], was applied to see whether this enzyme was required for econazole-induced Ca^{2+} release. Figure 5A shows that ATP (10 μM) induced a $[Ca^{2+}]_i$ rise of 35 nM ± 2 nM ($n = 3$). ATP is a phospholipase C-dependent agonist for $[Ca^{2+}]_i$ rise in most cells [Trautmann, 2009]. Figure 5B shows that incubation with 2 μM U73122

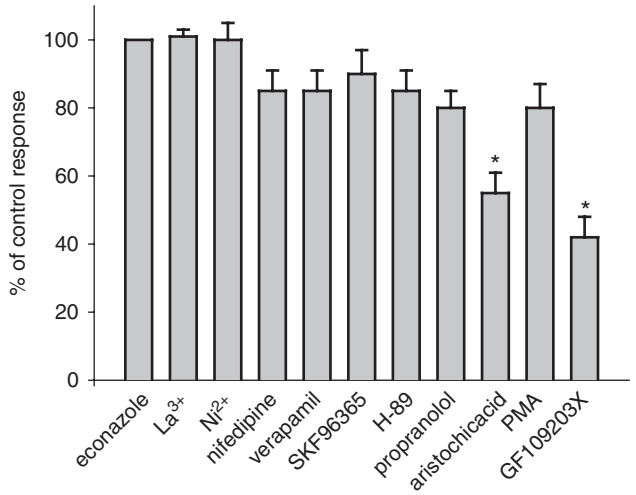

Fig. 3. Effect of modulators of protein kinases C and blockers of Ca^{2+} channels on econazole-induced $[Ca^{2+}]_i$ rise. Experiments were performed in Ca^{2+}-containing medium. La^{3+} (50 μM), Ni^{2+} (10 μM), nifedipine (1 μM), verapamil (1 μM), SK&F969365 (5 μM), H-89 (10 μM), propranolol (100 μM), aristolochic acid (20 μM), PMA (10 nM), and GF 109203X (2 μM) was added 1 min before addition of 30 μM econazole for 200 s. Data are expressed as the percentage of control. Control is the area under the curve of 30 μM econazole-induced $[Ca^{2+}]_i$ rise in the absence of pretreatment of any chemicals. Data are mean ± SEM of three experiments. $^*P<0.05$.

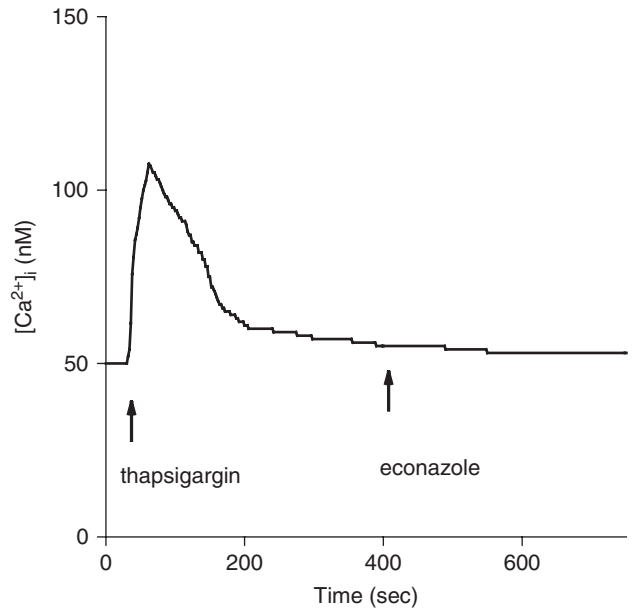

Fig. 4. Intracellular Ca^{2+} stores of econazole-induced Ca^{2+} release. In Ca^{2+}-free medium, thapsigargin (1 μM), and econazole (30 μM) were added at time points indicated. Data are typical of several experiments.

did not alter basal $[Ca^{2+}]_i$ but abolished ATP-induced $[Ca^{2+}]_i$ rise suggesting that U73122 effectively suppressed phospholipase C activity. U73343, an inactive U73122 analog, failed to affect ATP-induced $[Ca^{2+}]_i$

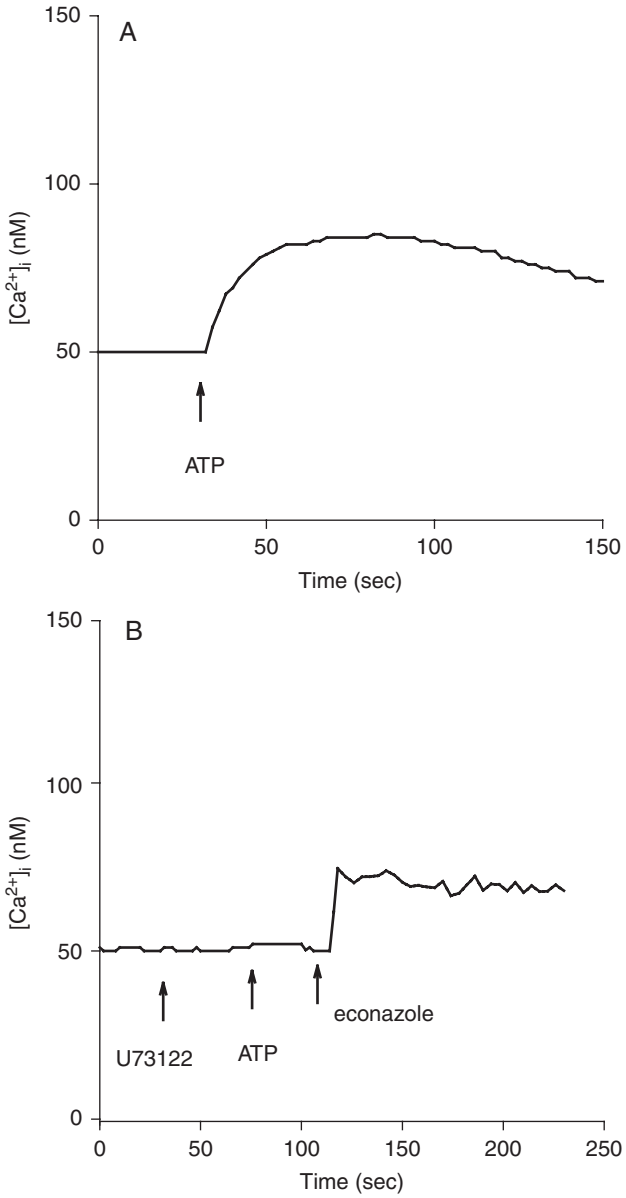

Fig. 5. Effect of U73122 on econazole-induced Ca^{2+} release. Experiments were performed in Ca^{2+}-free medium. **A:** ATP (10 μM) was added as indicated. **B:** U73122 (2 μM), ATP (10 μM), and econazole (30 μM) were added as indicated. Data are typical of several experiments.

rise ($n = 3$; not shown). Figure 5B also shows that addition of econazole (30 μM) after U73122 and ATP treatments caused a $[Ca^{2+}]_i$ rise of 24 ± 2 nM ($n = 3$), which was smaller than the control econazole response (Fig. 1B; 95 nM) by 75% ($P<0.05$).

Effect of Econazole on Cell Viability

Given that acute incubation with econazole induced a substantial and lasting $[Ca^{2+}]_i$ rise, and that an unregulated $[Ca^{2+}]_i$ rise often alters cell viability [Berridge,

2006], experiments were performed to examine the effect of overnight incubation with econazole on viability of OC2 cells. Cells were treated with 0–70 μM econazole overnight, and the tetrazolium assay was performed. In the presence of 10–70 μM econazole, cell viability decreased in a concentration-dependent manner (Fig. 6A).

Relationship Between Econazole-Induced $[Ca^{2+}]_i$ Rise and Cell Death

The next issue was whether the econazole-induced cytotoxicity was related to a preceding $[Ca^{2+}]_i$ rise.

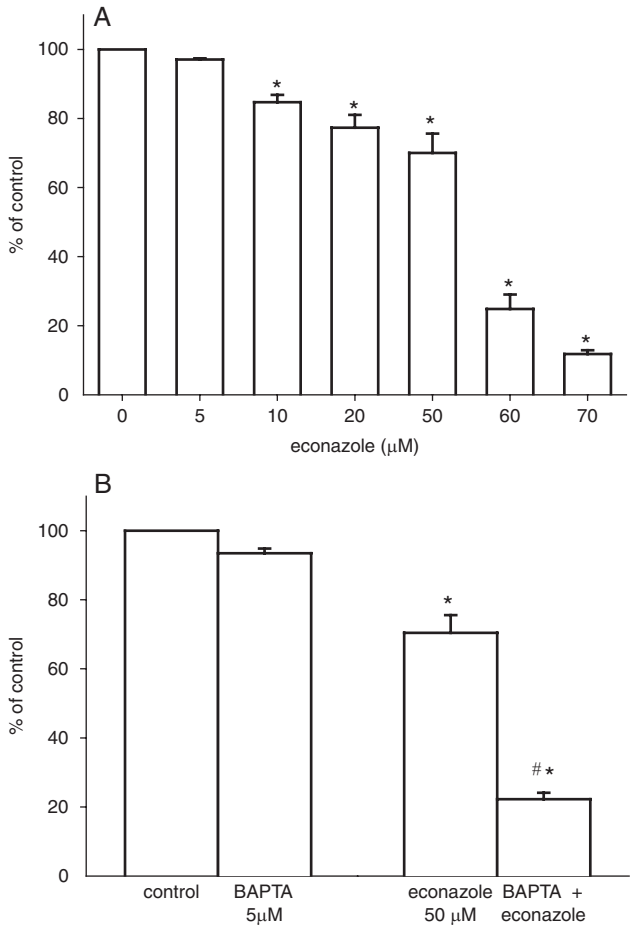

Fig. 6. Tetrazolium assay of the effect of econazole on viability of OC2 cells. **A:** Cells were treated with 0–70 μM of econazole overnight, and the tetrazolium assays were performed as described in Methods. Data are mean ±SEM of three experiments. Each treatment had 6 replicates (wells). Data are expressed as percentage of control that is the increase in cell number in econazole-free groups. Controls had 10,569±987 cells/well at the initiation of the experiments, and had 13,875±745 cells/well after overnight incubation. *$P<0.05$ compared with the first column from the left. **B:** Relationship between econazole-induced cell death and preceding $[Ca^{2+}]_i$ rises. The Ca^{2+} chelator BAPTA/AM (5 μM) was added to fura-2-loaded cells as described in Methods. BAPTA/AM loading did not significantly alter control cell growth. *$P<0.05$ compared with control (1st column from the left). ♯$P<0.05$ compared with the 3rd column.

The intracellular Ca^{2+} chelator BAPTA/AM [Tsien, 1980] was used to prevent a $[Ca^{2+}]_i$ rise during econazole pretreatment. Figure 6B shows that BAPTA/AM loading did not significantly alter control cell viability. In the presence of 50 μM econazole, BAPTA loading worsened econazole-induced cell death ($n = 3$; $P<0.05$).

Possible Role of ERK MAPK in Econazole-Induced Cell Death

Since a $[Ca^{2+}]_i$ rise did not contribute to econazole-induced cell death, the role of mitogen-activated protein kinase (MAPKs) were explored. PD98059 (ERK inhibitor; 10 μM), SP600125 (JNK inhibitor; 10 μM), and SB203580 (p38 MAPK inhibitor; 10 μM) were applied to see whether they prevented econazole-induced cell death. Because SP600125 and SB203580 considerably reduced cell viability in the absence of econazole ($n = 3$; not shown), they were not suitable for this experiment. In contrast, Figure 7 shows that PD98059 did not alter control viability but enhanced 20 μM econazole-induced cell death by 34% ($n = 3$; $P<0.05$).

Possible Involvement of Apoptosis in Econazole-Induced Cell Death

The percentage of cells that underwent apoptosis was analyzed by flow cytometry via measuring sub-diploidy nuclei, a hallmark of apoptosis, after cells were treated with 0–70 μM econazole overnight. As shown in Figure 8, apoptosis was observed in 10–70 μM econazole-treated groups. The subG1 phase was 1.9±0.2% ($n = 3$; $P<0.05$) in controls. After

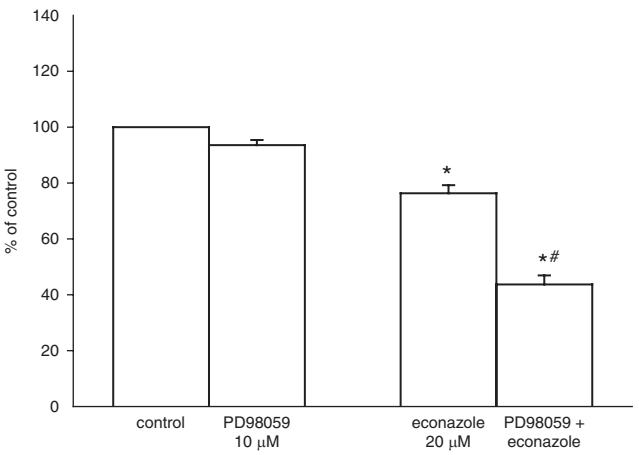

Fig. 7. Effect of inhibition of ERK MAPK on econazole-induced cell death. Cells were treated with vehicle (control), 10 μM PD98059, 20 μM econazole or PD98059/econazole, respectively, overnight before assessment of cell viability. *$P<0.05$ compared with control. ♯$P<0.05$ compared with the 3rd bar. Data are mean±SEM of three experiments. Each treatment had six replicates (wells).

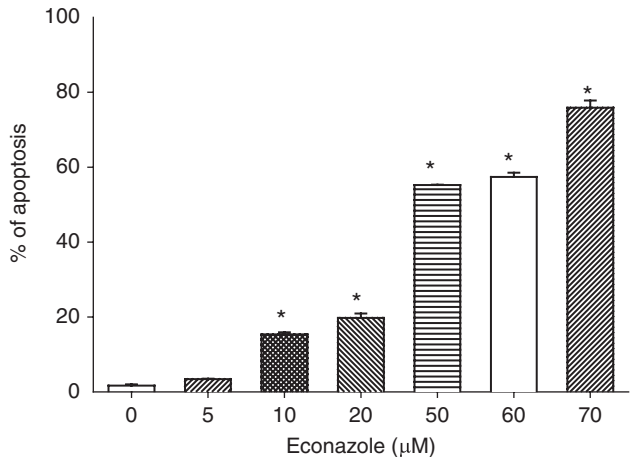

Fig. 8. Econazole-induced apoptosis. After treatment with 0–70 μM econazole for 24 h, cells were examined for apoptosis by using flow cytometry. Data are the mean ± SEM of three experiments. $^*P < 0.05$ as compared with control (without econazole).

incubation with 10–75 μM econazole, subG1 phase increased in a concentration-dependent manner.

DISCUSSION

Ca^{2+} handling has a key role in the physiology of nearly all cell types including oral cancer cells [Bootman et al., 2001]. The involvement of Ca^{2+} in oral cell function has been demonstrated. Berberine induced apoptosis in human HSC-3 oral cancer cells, which was mediated by simultaneous activation of the death receptor-mediated and mitochondrial pathway that was accompanied by a $[Ca^{2+}]_i$ rise [Lin et al., 2007]. The present study is the first to demonstrate that econazole caused $[Ca^{2+}]_i$ rise and death in OC2 human oral cancer cells. The data suggest that econazole increased $[Ca^{2+}]_i$ by depleting intracellular Ca^{2+} stores and causing Ca^{2+} influx from the extracellular milieu, since removing extracellular Ca^{2+} reduced a part of econazole-induced $[Ca^{2+}]_i$ rise. Removal of extracellular Ca^{2+} reduced the econazole response throughout the measurement, suggesting that Ca^{2+} influx occurred during the complete stimulation period. The econazole-induced Ca^{2+} influx in OC2 cells appears to be mediated by non-L-type Ca^{2+} channels in a PKC- and phospholipase A_2-dependent manner. Previous evidence showed that L-type Ca^{2+} channels might exist in OC2 cells [Huang et al., 2009]. Our data show that inhibition of PKC decreased econazole-induced Ca^{2+} signal, whereas OKC activation had no effect. PKC activity can regulate Ca^{2+} signals. Ashida et al. [2008] showed that Ca^{2+} oscillation induced by $P2Y_2$ receptor activation was regulated by a neuron-specific subtype of PKC (gammaPKC). Rathore et al. [2008] reported that hypoxia activated NADPH oxidase to increase $[Ca^{2+}]_i$ through the mitochondrial PKC signaling axis in pulmonary artery smooth muscle cells. Phospholipase A2 activity is associated with Ca^{2+} fluxes. Tedesco et al. [2009] show that snake PLA2 neurotoxins induced Ca^{2+} overload in nerve terminals of cultured neurons. Lupescu et al. [2006] suggest that human parvovirus B19 capsid protein VP1-induced Ca^{2+} entry was inhibited when phospholipase A2 activity was suppressed. Another possible mechanism that might contribute to the econazole-induced $[Ca^{2+}]_i$ rise is that econazole inhibited plasma membrane Ca^{2+}ATP pump so that Ca^{2+} could not be pumped out of the cells and $[Ca^{2+}]_i$ would rise via leaks in the plasma membrane. Whether econazole-induced Ca^{2+} entry was mediated by store-operated Ca^{2+} channels was uncertain since SK&F96365, a presumed inhibitor of store-operated Ca^{2+} entry [Mason et al., 1993; Abad et al., 2008], failed to affect econazole-induced $[Ca^{2+}]_i$ rise. Higher concentrations of SK&F96365 (5–20 μM) were tested; however, basal $[Ca^{2+}]_i$ was elevated significantly by these treatments. SK&F96365 has been shown to cause $[Ca^{2+}]_i$ rise in other cell types [Jan et al., 1999b]. The lack of inhibition of La^{3+} and Ni^{2+} on econazole-induced Ca^{2+} response could be because these metals not only inhibited Ca^{2+} influx but also inhibited Ca^{2+} efflux through the plasma membrane Ca^{2+} pump [Park et al., 1996] and thus, masked the inhibitory effect on Ca^{2+} influx. Whether OC2 cells possess L-type Ca^{2+} channels is unclear. A previous report showed that nifedipine inhibited safrole (a carcinogen)-induced $[Ca^{2+}]_i$ rise in OC2 cells [Huang et al., 2005]. In the present study, L-type Ca^{2+} channel blockers failed to affect econazole-induced Ca^{2+} signal. Furthermore, PKA and phospholipase D did not appear to play a role because H-89 and propranolol did not affect the econazole response. Activation of phospholipase C produces IP_3 and diacylglycerol, which activates PKC. Thus the result that econazole-induced $[Ca^{2+}]_i$ rise was inhibited by inhibition of PKC implicates a role of phospholipase C in econazole-induced response.

Regarding the Ca^{2+} stores involved in econazole-induced Ca^{2+} release, the thapsigargin-sensitive stores might be the dominant store responsible for econazole-induced Ca^{2+} release as thapsigargin pretreatment abolished the econazole-induced $[Ca^{2+}]_i$ rise. Consistent with the PKC data, it appears that phospholipase C-dependent pathways played a significant role in econazole-induced Ca^{2+} release, since the response was substantially reduced when phospholipase C activity was suppressed.

Econazole is toxic to several cell lines including human colon cancer cells [Ho et al., 2005] and mouse lymphoma and human *T*-cell leukemia cells [Zisterer

et al., 1997]. In the present study, econazole was cytotoxic to OC2 oral cancer cells in a concentration-dependent manner. Ca^{2+} overloading can initiate processes leading to alterations in cell viability [Berridge, 2006]. As econazole induced $[Ca^{2+}]_i$ rises and cell death, it was of interest whether the death occurred in a Ca^{2+}-dependent manner. Our data show that the econazole-induced cell death was even enhanced by preventing econazole-induced $[Ca^{2+}]_i$ rise. This implies that in this case, econazole-induced cell death was not triggered by a $[Ca^{2+}]_i$ rise. Emptying of intracellular Ca^{2+} stores and/or influx of extracellular Ca^{2+} can modulate cell viability in many cells [Clapham, 1995]. However, Ca^{2+}-independent cell death occurs in some cells (e.g., thymic lymphoma cells) [Matuszyk et al., 1998] and neutrophils [Das, 1999]. MAPKs play a pivotal role in various cellular responses, including proliferation and apoptosis [Blüthgen and Legewie, 2008]. Thus, we explored whether ERK, JNK, and p38 MAPKs were involved in econazole-induced cell death. Our results suggest a possible role of ERK MAPK in the cytotoxicity of econazole. However, the increase in cell death seen in the study may also be due to cumulative effect of inhibitor and econazole. Additionally, econazole-induced cell death involved apoptosis as based on propidium iodide staining, consistent with the apoptotic effect of econazole observed in other cells [Sobecks et al., 1996; Ho et al., 2005].

Collectively, the present data show that econazole induced Ca^{2+} release and Ca^{2+} influx, and evoked non-Ca^{2+}-triggered, ERK MAPK-related apoptosis in OC2 human oral cancer cells. As a rise in $[Ca^{2+}]_i$ can interfere with many cellular processes, caution should be taken in using econazole for other in vitro studies, and it should be noted that econazole at concentrations of $>10\,\mu M$ may be apoptotic.

ACKNOWLEDGMENTS

This work was supported in part by grants from Veterans General Hospital-Kaohsiung (VGHKS98–100) (to C.R. Jan).

REFERENCES

Abad E, Lorente G, Gavara N, Morales M, Gual A, Gasull X. 2008. Activation of store-operated Ca^{2+} channels in trabecular meshwork cells. Invest Ophthalmol Vis Sci 49:677–686.

Ashida N, Ueyama T, Rikitake K, Shirai Y, Eto M, Kondoh T, Kohmura E, Saito N. 2008. Ca^{2+} oscillation induced by P2Y2 receptor activation and its regulation by a neuron-specific subtype of PKC (gammaPKC). Neurosci Lett 446:123–128.

Berridge MJ. 2006. Calcium microdomains: organization and function. Cell Calcium 40:405–412.

Blüthgen N, Legewie S. 2008. Systems analysis of MAPK signal transduction. Essays Biochem 45:95–107.

Bootman MD, Lipp P, Berridge MJ. 2001. The organisation and functions of local $[Ca^{2+}]_i$ signals. J Cell Sci 114:2213–2222.

Chang HT, Liu CS, Chou CT, Hsieh CH, Chang CH, Chen WC, Liu SI, Hsu SS, Chen JS, Jiann BP, Huang JK, Jan CR. 2005. Econazole induces increases in free intracellular Ca^{2+} concentrations in human osteosarcoma cells. Hum Exp Toxicol 24:453–458.

Chu ST, Huang CC, Huang CJ, Cheng JS, Chai KL, Cheng HH, Fang YC, Chi CC, Su HH, Chou CT, Jan CR. 2007. Tamoxifen-induced $[Ca^{2+}]_i$ rises and Ca^{2+}-independent cell death in human oral cancer cells. J Receptor Signal Transduct Res 27:353–367.

Clapham DE. 1995. Intracellular calcium. Replenishing the stores. Nature 375:634–635.

Das S, Bhattacharyya S, Ghosh S, Majumdar S. 1999. TNF-alpha induced altered signaling mechanism in human neutrophil. Mol Cell Biochem 197:97–108.

Davies R, Hayat S, Wigley CB, Robbins J. 2004. The calcium influx pathway in rat olfactory ensheathing cells shows TRPC channel pharmacology. Brain Res 1023:154–156.

Florcruz NV, Peczon Jr I. 2008. Medical interventions for fungal keratitis. Cochrane Database Sys Rev 1:CD004241.

Grynkiewicz G, Poenie M, Tsien RY. 1985. A new generation of Ca^{2+} indicators with greatly improved fluorescence properties. J Biol Chem 260:3440–3450.

Heath-Engel HM, Chang NC, Shore GC. 2008. The endoplasmic reticulum in apoptosis and autophagy: role of the BCL-2 protein family. Oncogene 27:6419–6433.

Ho YS, Wu CH, Chou HM, Wang YJ, Tseng H, Chen CH, Chen LC, Lee CH, Lin SY. 2005. Molecular mechanisms of econazole-induced toxicity on human colon cancer cells: G0/G1 cell cycle arrest and caspase 8-independent apoptotic signaling pathways. Food Chem Toxicol 43:1483–1495.

Huang CC, Huang CJ, Cheng JS, Liu SI, Chen IS, Tsai JY, Chou CT, Tseng PL, Jan CR. 2009. Fendiline-evoked $[Ca^{2+}]_i$ rises and non-Ca^{2+}-triggered cell death in human oral cancer cells. Hum Exp Toxicol 28:41–48.

Huang JK, Huang CJ, Chen WC, Liu SI, Hsu SS, Chang HT, Tseng LL, Chou CT, Chang CH, Jan CR. 2005. Independent $[Ca^{2+}]_i$ increases and cell proliferation induced by the carcinogen safrole in human oral cancer cells. Naunyn Schmiedebergs Arch Pharmacol 372:88–94.

Jacobsen J, Bjerregaard S, Pedersen M. 1999. Cyclodextrin inclusion complexes of antimycotics intended to act in the oral cavity — drug supersaturation, toxicity on TR146 cells and release from a delivery system. Eur J Pharmacol Biopharmacol 48:217–224.

Jan CR, Ho CM, Wu SN, Tseng CJ. 1999a. Multiple effects of econazole on calcium signaling: depletion of thapsigargin-sensitive calcium store, activation of extracellular calcium influx, and inhibition of capacitative calcium entry. Biochim Biophys Acta 1448:533–542.

Jan CR, Ho CM, Wu SN, Tseng CJ. 1999b. Multiple effects of 1-[beta-[3-(4-methoxyphenyl)propoxy]-4-methoxyphenethyl]-1H-imidazole hydrochloride (SKF 96365) on Ca^{2+} signaling in MDCK cells: depletion of thapsigargin-sensitive Ca^{2+} store followed by capacitative Ca^{2+} entry, activation of a direct Ca^{2+} entry, and inhibition of thapsigargin-induced capacitative Ca^{2+} entry. Naunyn Schmiedebergs Arch Pharmacol 359:92–101.

Jiang N, Zhang ZM, Liu L, Zhang C, Zhang YL, Zhang ZC. 2006. Effects of Ca^{2+} channel blockers on store-operated Ca^{2+} channel currents of Kupffer cells after hepatic ischemia/reperfusion injury in rats. World J Gastroenterol 12:4694–4698.

Koch BD, Faurot GF, Kopanitsa MV, Swinney DC. 1994. Pharmacology of a Ca^{2+}-influx pathway activated by emptying the intracellular Ca^{2+} stores in HL-60 cells: evidence that a cytochrome P-450 is not involved. Biochem J 302:187–190.

Lin CC, Yang JS, Chen JT, Fan S, Yu FS, Yang JL, Lu CC, Kao MC, Huang AC, Lu HF, Chung JG. 2007. Berberine induces apoptosis in human HSC-3 oral cancer cells via simultaneous activation of the death receptor-mediated and mitochondrial pathway. Anticancer Res 27:3371–3378.

Lovborg H, Gullbo J, Larsson R. 2005. Screening for apoptosis-classical and emerging techniques. Anticancer Drugs 16:593–599.

Lupescu A, Bock CT, Lang PA, Aberle S, Kaiser H, Kandolf R, Lang F. 2006. Phospholipase A2 activity-dependent stimulation of Ca^{2+} entry by human parvovirus B19 capsid protein VP1. J Virol 80:11370–11380.

Mason MJ, Mayer B, Hymel LJ. 1993. Inhibition of Ca^{2+} transport pathways in thymic lymphocytes by econazole, miconazole, and SKF 96365. Am J Physiol 264:C654–C662.

Matuszyk J, Kobzdej M, Ziolo E, Kalas W, Kisielow P, Strzadala L. 1998. Thymic lymphomas are resistant to Nur77-mediated apoptosis. Biochem Biophys Res Commun 249:279–282.

McLean KJ, Marshall KR, Richmond A, Hunter IS, Fowler K, Kieser T, Gurcha SS, Besra GS, Munro AW. 2002. Azole antifungals are potent inhibitors of cytochrome P450 mono-oxygenases and bacterial growth in mycobacteria and streptomycetes. Microbiol 148:2937–2949.

Merritt JE, Jacob R, Hallam TJ. 1989. Use of manganese to discriminate between calcium influx and mobilization from internal stores in stimulated human neutrophils. J Biol Chem 264:1522–1527.

Orrenius S, Nicotera P. 1994. The calcium ion and cell death. J Neural Transm 43(suppl):1–11.

Park YB, Herrington J, Babcock DF, Hille B. 1996. Ca^{2+} clearance mechanisms in isolated rat adrenal chromaffin cells. J Physiol 492:329–346.

Rathore R, Zheng YM, Niu CF, Liu QH, Korde A, Ho YS, Wang YX. 2008. Hypoxia activates NADPH oxidase to increase $[ROS]_i$ and $[Ca^{2+}]_i$ through the mitochondrial ROS-PKCepsilon signaling axis in pulmonary artery smooth muscle cells. Free Rad Biol Med 45:1223–1231.

Rizzuto R, Marchi S, Bonora M, Aguiari P, Bononi A, De Stefani D, Giorgi C, Leo S, Rimessi A, Siviero R, Zecchini E, Pinton P. 2009. Ca^{2+} transfer from the ER to mitochondria: when, how and why. Biochim Biophys Acta 1787:1342–1351.

Salido GM, Sage SO, Rosado JA. 2009. TRPC channels and store-operated Ca^{2+} entry. Biochim Biophys Acta 1793:223–230.

Sobecks R, McCormick TS, Distelhorst CW. 1996. Imidazole antifungals Miconazole and Econazole induce apoptosis in mouse lymphoma and human T cell leukemia cells: regulation by Bcl-2 and potential role of calcium. Cell Death Differ 3:331–337.

Tedesco E, Rigoni M, Caccin P, Grishin E, Rossetto O, Montecucco C. 2009. Calcium overload in nerve terminals of cultured neurons intoxicated by alpha-latrotoxin and snake PLA2 neurotoxins. Toxicon 54:138–144.

Thastrup O, Cullen PJ, Drøbak BK, Hanley MR, Dawson AP. 1990. Thapsigargin, a tumor promoter, discharges intracellular Ca^{2+} stores by specific inhibition of the endoplasmic reticulum Ca^{2+}-ATPase. Proc Natl Acad Sci USA 87:2466–2470.

Thompson AK, Mostafapour SP, Denlinger LC, Bleasdale JE, Fisher SK. 1991. The aminosteroid U-73122 inhibits muscarinic receptor sequestration and phosphoinositide hydrolysis in SK-N-SH neuroblastoma cells. A role for Gp in receptor compartmentation. J Biol Chem 266:23856–23862.

Trautmann A. 2009. Extracellular ATP in the immune system: more than just a danger signal. Sci Signal 2:pe6.

Tsien RY. 1980. New calcium indicators and buffers with high selectivity against magnesium and protons: design, synthesis, and properties of prototype structures. Biochem 19:2396–2404.

Vanden Bossche H, Engelen M, Rochette F. 2003. Antifungal agents of use in animal health—chemical, biochemical and pharmacological aspects. J Vet Pharmacol Ther 26:5–29.

Zisterer DM, Williams DC. 1997. Calmidazolium and other imidazole compounds affect steroidogenesis in Y1 cells: lack of involvement of the peripheral-type benzodiazepine receptor. J Steroid Biochem Mol Biol 60:189–195.